Decadal Changes in the Atmospheric Circulation and Associated Surface Climate Variations in the Northern Hemisphere Winter

MASAHIRO WATANABE AND TSUYOSHI NITTA

Center for Climate System Research, University of Tokyo, Tokyo, Japan

(Manuscript received 28 May 1997, in final form 20 March 1998)

ABSTRACT

This study attempts to investigate decadal-scale climate changes in the mid- and high latitudes of the Northern Hemisphere in winter 1989 by using various observational data for atmospheric parameters, sea surface temperature (SST), and snow cover.

Decadal-scale changes in the winter atmosphere after 1989 are characterized as follows: a dipole pattern of height anomalies between midlatitudes and polar regions with an equivalent barotropic structure, temperature changes with cooling in the polar region and warming in midlatitudes in the middle troposphere, and associated reduction of the subtropical jet stream. Statistical tests applied to the 500-hPa height field reveal that the changes in 1989 are a distinct discontinuity or shift on the decadal scale with hemispheric extent. The spatial structure is interpreted as a linear combination of three teleconnections: the North Atlantic oscillation, Pacific–North American, and Eurasian patterns, in addition to the zonally symmetric dipole. On the other hand, the sharpness of decadal changes in 1989 arises from synchronous phase shifts of interdecadal variations over the Pacific Ocean and quasi-decadal variations over the North Atlantic. Similar concurrence is also found in winter 1977. In agreement with previous studies, the interdecadal atmospheric variations over the North Pacific reveal a strong coupling with tropical/extratropical SST anomalies in the Pacific Ocean. A relationship between the quasi-decadal variability of the North Atlantic atmosphere and underlying SST anomalies is relatively tenuous.

Surface air temperatures show a warming over all of Eurasia after winter 1989. It is shown by the analysis of snow cover in the Northern Hemisphere derived from NOAA satellites that a large decrease (increase) of the snow extent over the eastern part of the Eurasian continent occurred in autumn 1988 (1976) prior to winter 1989 (1977). It is suggested that the anomalies in the Eurasian snow cover during autumn play a role as an amplifier in the atmospheric shifts. These snow anomalies may be as important for the atmospheric changes as changes in SSTs.

1. Introduction

Climate variations on decadal to interdecadal timescales have received much attention in the last decade. Remarkable progress in the examination of the decadal/interdecadal climate changes has been made due to accumulation of observational data and recent development of general circulation models (GCMs) of the atmosphere and ocean. However, there still remain some uncertain subjects in our understanding of decadal/interdecadal variabilities, for example, the mechanism of variations.

Over the Pacific Ocean, an El Niño–Southern Oscillation (ENSO)-like interdecadal variability is dominant in the Tropics and extratropics (Zhang et al. 1997, and references therein). The Pacific interdecadal variations are characterized by the warming (cooling) of sea surface temperatures (SSTs) in the tropical central-eastern Pacific (central North Pacific) since the late 1970s (Nitta and Yamada 1989; Tanimoto et al. 1993; Kawamura 1994) and the intensified Pacific–North American (PNA) teleconnection pattern in the troposphere (Trenberth 1990; Trenberth and Hurrell 1994). Trenberth and Hurrell (1994) and Graham (1994) concluded, by using respectively observations and an atmospheric GCM (AGCM), that the cooling in SSTs in the North Pacific and concomitant deepening of the Aleutian low are linked to the warming in SSTs in the tropical central-eastern Pacific. On the other hand, Latif and Barnett (1994, 1996) proposed another scenario for the North Pacific interdecadal variations that does not need a forcing from the Tropics. Anyhow, these diagnostics strongly suggest that the decadal changes in SSTs over the Pacific Ocean and Northern Hemisphere winter atmosphere are strongly coupled with each other.

Over the Atlantic Ocean, on the other hand, diagnostic studies of the decadal variability have been made by Deser and Blackmon (1993) and Kushnir (1994). Deser and Blackmon (1993) found two modes of variability

Corresponding author address: M. Watanabe, Center for Climate System Research, University of Tokyo, 4-6-1 Komaba, Meguro-ku, Tokyo 153, Japan.
E-mail: hiro@ccsr.u-tokyo.ac.jp

on decadal/interdecadal timescales in surface climate fields. One has an irregular periodicity between 9 and 12 yr and a north–south dipole pattern in SSTs while the other represents a longer timescale fluctuation. They speculated that the latter is associated with the strength of the thermohaline circulation in the Atlantic Ocean. This interdecadal variability is also found by Kushnir (1994), with a corroboration of the earlier result by Bjerknes (1964); however, it is out of the focus of this study. On the other hand, the decadal variations found by Deser and Blackmon (1993) may be related to our findings, as shown in section 4.

Quite recently, decadal-scale changes that may have characteristics different from known decadal variations are reported. First, Walsh et al. (1996) found that the northern polar vortex was persistently intensified after the 1988/89 winter. Their finding was further confirmed by Tanaka et al. (1996). In association with this change in polar atmospheric circulation, Maslanik et al. (1996) reported that the Arctic summer ice cover is decreasing in recent years. Also Tachibana et al. (1996) have shown that the sea ice extent in the southern Okhotsk Sea has been drastically decreasing since winter 1989. They discussed the relationship between the decrease in sea ice and recent continuous warm winters in Japan. These observational results describe large-scale changes mainly in higher latitudes; however, the hemispheric structure and mechanism of those changes have not been well documented yet.

The purpose of this study is to investigate the changes that occurred in winter 1989 and the associated decadal-scale atmospheric variations by using various observational datasets. The datasets used in this study are described in section 2. In section 3, spatial structures of decadal-scale atmospheric changes in winter 1989 are described over the entire Northern Hemisphere. Analyses are extended in section 4 to seek the relationship between the decadal changes in 1989 and two known decadal variations: the Pacific interdecadal and Atlantic decadal variations. Section 4 also offers results of the analysis for decadal-scale changes in 1989 in connection with surface conditions such as surface temperatures and snow cover. Observational results emphasize the importance of the autumn snow extent anomaly over the Eurasian continent on the atmospheric changes in winter 1989. The results are discussed and summarized in section 5.

2. Data

Various data for the atmosphere, ocean surface, and cryosphere on the global domain are used in this study. Atmospheric variables primarily consist of two datasets: the National Centers for Environmental Prediction (formerly the National Meteorological Center) operational analysis dataset and gridded data compiled by the Japan Meteorological Agency (JMA). The former contains monthly mean temperature, geopotential height, and corresponding geostrophic wind at 200-, 300-, 500-, and 700-hPa pressure levels. The data exist on a $5^\circ \times 5^\circ$ octagonal grid superimposed on a polar stereographic projection of the Northern Hemisphere north of 20°N, and are available from the 1950s or before (depending on the pressure level) to December 1994. The latter includes monthly mean sea level pressure (SLP) and 100-hPa geopotential height data, both on a $5^\circ \times 5^\circ$ grid of the Northern Hemisphere, and available from January 1951 to February 1995 for SLP and from January 1963 to February 1995 for 100-hPa height.

Global SST data consist of monthly mean SSTs with the spatial resolution of 2° on a latitude–longitude regular-rectangular mesh, compiled by JMA. The data over the latitudes extending from 80°N to 80°S for the period 1946–95 are available. These SST data are based on several different sources: Comprehensive Ocean-Atmosphere Data Set for 1946–69, National Oceanic and Atmospheric Administration (NOAA) dataset for 1970–84, and Oceanographical Division of JMA for 1985 onward. Quality of the data was discussed in Nitta and Yamada (1989).

Combined surface temperatures, compiled by P. D. Jones, were provided by the National Center for Atmospheric Research. The data consist of quality-controlled surface air temperatures over land and SSTs over oceans with a $5^\circ \times 5^\circ$ resolution from January 1854 to December 1994. Jones et al. (1986) give further description of the data.

Northern Hemisphere weekly snow cover data are used in this study for the diagnostic analysis. The snow cover data are derived from NOAA satellites and compiled at the National Environmental Satellite, Data and Information Service. The data consist of digitized (1/0) information that indicates the presence or absence of snow weekly, and have 89×89 grids equally spaced on a polar stereographic projection; that is, the spatial resolution varies with latitude. The available period of the data extends from November 1966 to December 1991; however, the pre-1972 data are excluded from the analysis because of some systematic errors (Wiesnet et al. 1987).

In the following sections, in which the above various data are examined, most of data are arranged as monthly or seasonal anomalies (3-month means such as December–February), which are obtained by subtracting the long-term averages from the data.

3. Abrupt changes in the atmosphere in 1989

As described in the introduction, it appeared that large changes in the Northern Hemisphere atmosphere occurred in winter 1989. For a preliminary understanding of the hemispheric spatial structures of these changes, differences for the period 1989–94 from the prior 6-yr average for several atmospheric variables in the Northern Hemisphere winter are shown in Fig. 1. Differences in the 500-hPa height fields (Fig. 1a) show that the

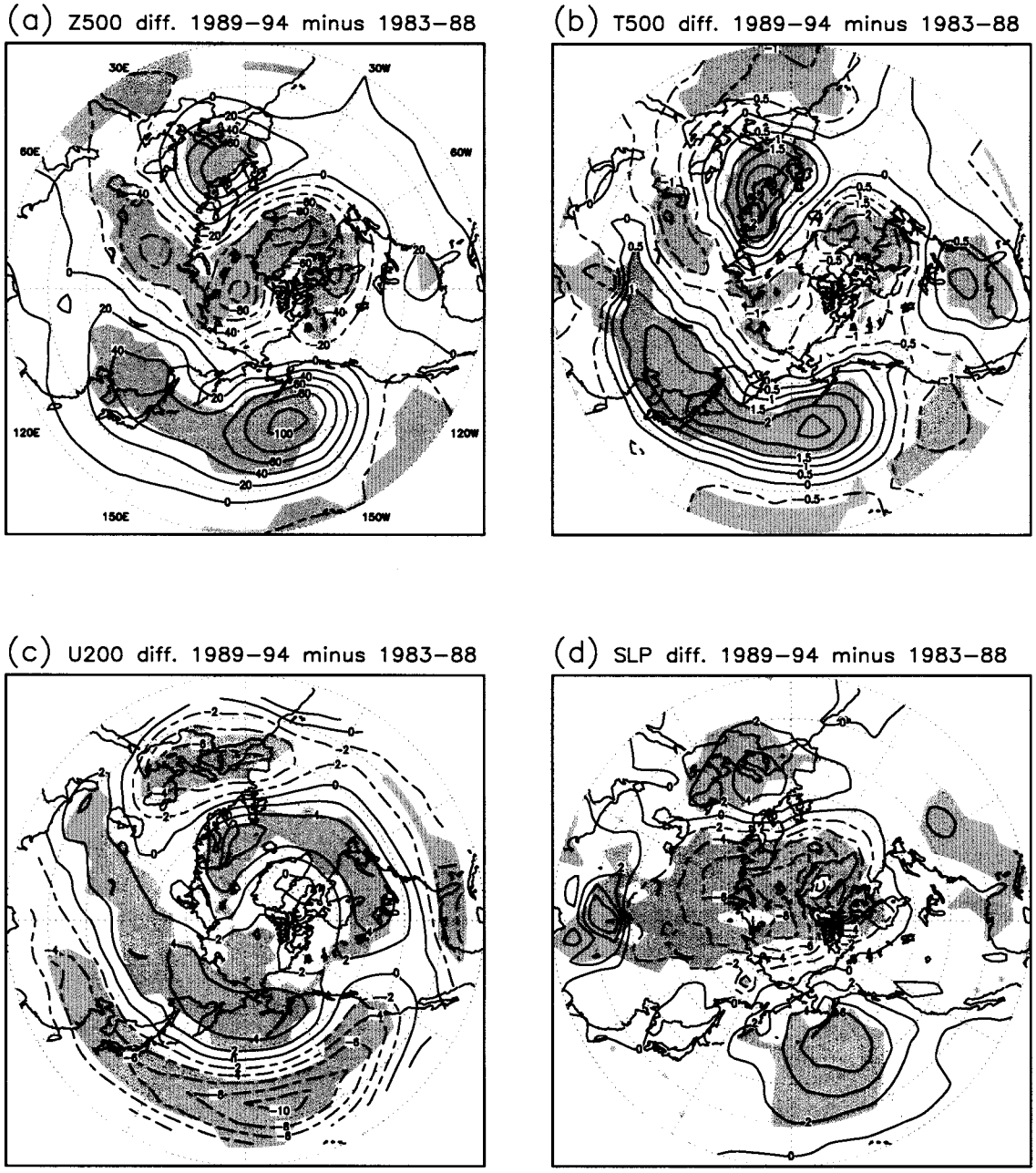

FIG. 1. Epoch differences 1989–94 mean less 1983–88 mean in Northern Hemisphere winter (a) 500-hPa heights, (b) 500-hPa temperature, (c) 200-hPa zonal wind, and (d) sea level pressure. Respective contour intervals are 20 m, 0.5 K, 1.5 m s^{-1}, and 1.5 hPa, and negative contours are dashed. Areas where *t* test exceeds 5% significance level are shaded.

changes are generally characterized by a dipole pattern of height anomalies between midlatitudes and polar regions. Moreover, not only the dipole but also several known teleconnection patterns, such as the North Atlantic oscillation (NAO), the PNA, and the Eurasian (EU) pattern, are dominant in Fig. 1a. Although the EU is the same as that found in Wallace and Gutzler (1981) or EU1 of Barnston and Livezey (1987), the NAO reveals a ''not classical'' pattern (Kimoto and Ghil 1993) due to the elongate subtropical anomalies [they are rather reminiscent of Barnston and Livezey's (1987) mode 2]. Results of the *t* test for 500-hPa height differences shows that significant shifts occurred in winter 1989 over large regions (37.3% of Northern Hemisphere north of 20°N). These patterns of 500-hPa height difference are quite similar (no phase tilt) with those at other pressure levels (e.g., 200, 300, 700 hPa) but the amplitude increases with height (figures are not shown).

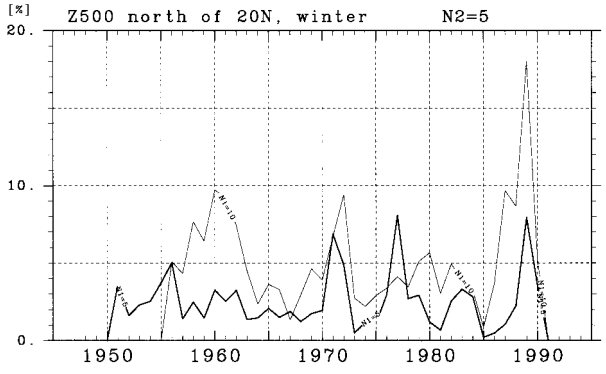

FIG. 2. Ratio (%) of areas that exceed 5% significance level when Lepage test is applied to winter 500-hPa geopotential height north of 20°N. The thick line indicates the result of $n1 = n2 = 5$, while the thin line represents the result for $n1 = 10$ and $n2 = 5$.

Thus, the changes in geopotential height fields indicate a strong, equivalent barotropic structure.

Changes in 500-hPa temperature (Fig. 1b) show a similar spatial structure to Fig. 1a: warming over midlatitude regions from eastern Eurasia to the North Pacific and from North America to Europe, and cooling over the polar region centered on the Labrador Sea and central Eurasia. With the constraint of the thermal wind relationship, subtropical jets over the Pacific and Atlantic are weakened as shown in 200-hPa zonal wind differences (Fig. 1c). Differences in SLP (Fig. 1d) also appear as a dipole pattern, although the centers of action are somewhat different from Figs. 1a and 1b. The zonally symmetric seesaw shown in Fig. 1d is known as one of the dominant major patterns in the SLP field during the Northern Hemisphere winter (Wallace and Gutzler, 1981; Trenberth and Paolino 1981).

The features shown in Fig. 1 strongly suggest that the changes in winter 1989 are decadal-scale shifts in the atmospheric circulation in the Northern Hemisphere. This point is further tested by using another statistical method. The test used here is the Lepage test, which was introduced by Yonetani (1992). This test judges a significant discontinuity between two independent series, having sample size of $n1$ and $n2$, based on the sum of the squares of the normalized Wilcoxon and Ansariy–Bradley statistics. In the Lepage test, the dependence of the result on the number of samples, $n1$ and $n2$, taken to calculate the test statistics remains as same as the t test, the difference between two averages. This leads to the necessity to confirm whether the result is robust for the alternative sampling size.

Figure 2 shows the results of the Lepage test for 500-hPa heights north of 20°N represented by ratios of areas significant at the 5% level for each year. Since the change in 1989 is focused on, and the data before 1994 are used, sample size of the latter period, $n2$, is fixed to 5. Both cases in Fig. 2 ($n1 = 5$ and $n1 = 10$) indicate that the change in winter 1989 was the most prominent in the recent four decades. That is, statistically significant shifts are observed over areas approximately 10% (20%) for $n1 = 5$ ($n1 = 10$) of the Northern Hemisphere north of 20°N in 1989. This result is robust even when $n1$ is changed to 15 or 20. Similar results are obtained from other fields such as temperature, zonal wind, and SLP (not shown).

Because of a small degree of freedom (see Yonetani 1992), the Lepage test leads to severe results for significance relative to the t test. Therefore, the results of Fig. 2 confirm the conclusion from Fig. 1 that the change in 1989 is a *hemispheric* shift in the atmosphere. Actually, when the t test is applied for $n1 = n2 = 5$ as in Fig. 2, 47.13% of the area in the Northern Hemisphere exceeds the 5% significance level. However, it is not clear whether this shift arises from a unique decadal variability or synchronous changes of different decadal-scale fluctuations.

4. Decadal climate variations in the mid- and high latitudes

As described in the previous section, decadal-scale changes in the atmospheric circulation observed in winter 1989 reveal a combined characteristic of several known teleconnections. In this section, the following questions associated with these changes are taken up.

- Are the shifts in 1989 a singular event, or part of decadal climate variations?
- What is the relation with known interdecadal/decadal modes dominant over the Pacific and Atlantic Oceans?
- How are the shifts in the atmosphere connected with surface climate fields?

The second question implies that one should examine the regionality of patterns in Fig. 1.

a. Atmospheric variability

An empirical orthogonal function (EOF), which is based on the temporal covariance matrix, is often used in statistical analyses of the climate variations. Here the EOF analysis is applied to winter 500-hPa height fields for the period 1946–94.

The leading EOF (EOF1) of winter 500-hPa heights accounts for 21.19% of the total variance, and the spatial pattern (Fig. 3) resembles the difference field associated with the decadal shift in 500-hPa heights (Fig. 1). Namely, the EOF1 reveals a north–south dipole structure that involves teleconnection patterns of the NAO, PNA, and EU. This resemblance is further supported by the temporal variations of the EOF1. The principal components (PCs) indicate that low pressure anomalies in high latitudes centered on Greenland, and high pressure anomalies over areas from eastern Eurasia to the North Pacific and from the western Atlantic to Europe, are intensified in 1989 and maintained afterward. These features, consistent with results obtained in the previous section, imply that the EOF1 of 500-hPa heights represents the

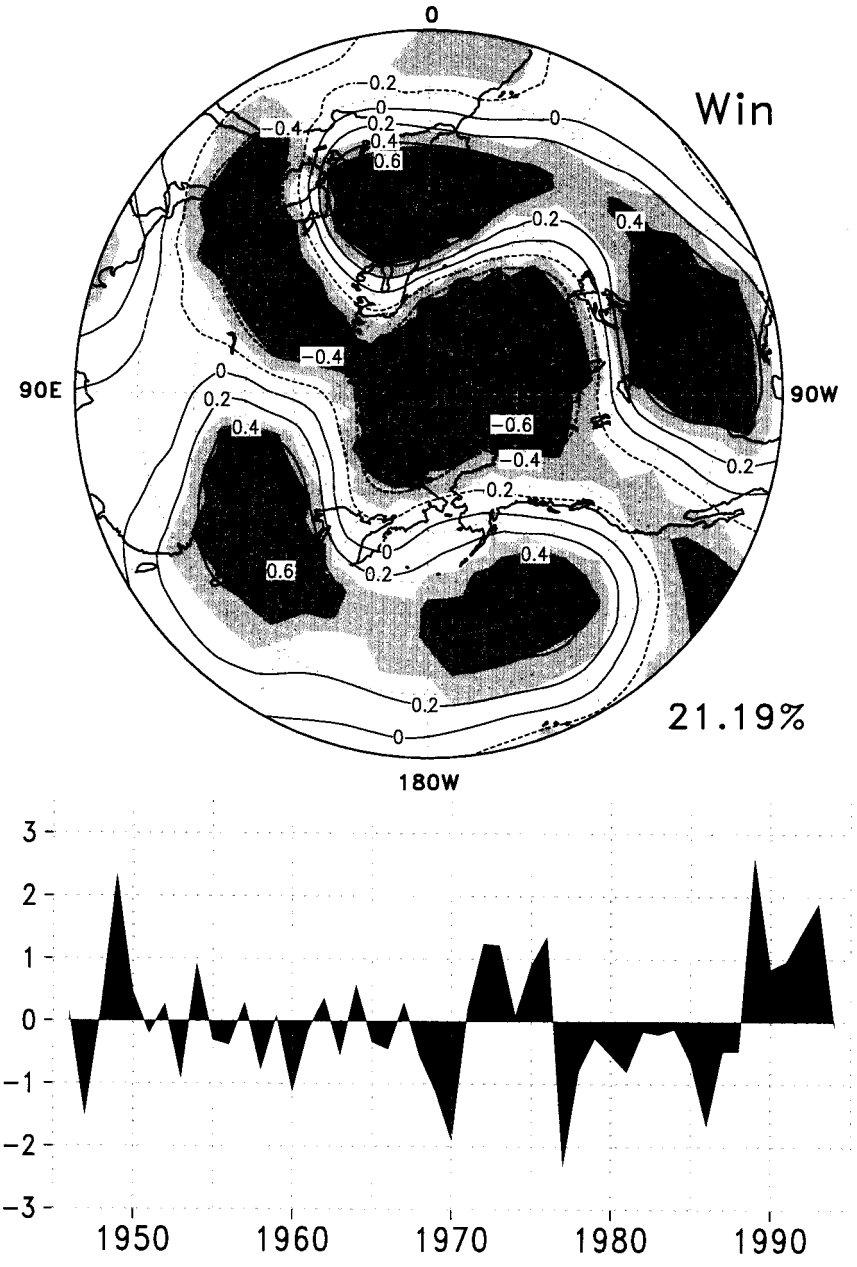

FIG. 3. (top) Spatial pattern of the leading EOF of winter 500-hPa height north of 20°N, based on 49-yr fields from 1946 to 1994, and (bottom) its principal components (PCs). In the upper panel, correlation coefficients of the PCs with 500-hPa heights are plotted instead of eigenvectors, and areas having significant correlations at the 5% (1%) level are light (dark) shaded. The number at the right of the upper panel indicates the percentage of the total variance explained by this mode.

decadal shift that occurred in 1989. It is noticeable that, at least after 1970, decadal variations and additional positive trends are dominant in the EOF1 mode: positive periods for the early 1970s and after 1989, and negative periods from the late 1970s to 1980s. At years when abrupt shifts are observed in leading PCs (i.e., 1971 and 1977), the spatial significance of decadal discontinuity becomes large in Fig. 2. A prevalence of the dipole anomalies on these longer timescales is consistent with results by Kushnir and Wallace (1989). High correlations are found between PCs of the EOF1 and geopotential height fields at several pressure levels (figures are not shown). This suggests that this mode of variability contains a strong barotropic characteristic through the troposphere to the lower stratosphere.

In order to examine the regionality of EOFs, an or-

thogonal rotation based on the varimax criterion (Richman 1986) is often applied to leading EOFs. In this case, because a sampling error estimation of North et al. (1982) indicates that the EOF1 is not independent of the following EOFs, the rotation may be effective and lead to more robust patterns, statistically (Cheng et al. 1995). However, we used here a different method to identify the regional structure contained in the EOF1: the EOF analysis to ''residual'' fields, in which the coherent variability with a specific teleconnection is eliminated. It should be noted that the varimax rotation to the leading 10 EOFs yields results similar to the following figures (not shown).

For indicators of tropospheric pressure variability over the North Pacific and North Atlantic, we employed the North Pacific (NP) index (Trenberth and Hurrell 1994) and the NAO index (Hurrell 1995), which are based on the gridded mean sea level pressure (SLP) data. Unlike in Hurrell (1995), the NAO index is computed using the nonnormalized SLP anomalies in order to compare with the NP index:

$$\mathrm{NAO} = \frac{1}{2}[p^*(10\mathrm{W}, 40\mathrm{N}) - p^*(20\mathrm{W}, 65\mathrm{N})],$$

where p^* denotes the winter SLP anomaly at a grid point. The residual field is defined by subtracting the linear projection of the NP or NAO indices onto the field, and conventionally referred to as the NP-removed or NAO-removed field. Figure 4a shows the leading EOF (15.51%) of NP-removed 500-hPa heights and the corresponding PCs superimposed on the NAO indices. It is evident that two time series well resemble each other and are highly correlated (+0.624, which is significant at 1% level) because of a coherent decadal variability. The spatial pattern of the leading EOF shown in Fig. 4a reveals a north–south dipole similar to that in Fig. 3, but the signals over the North Pacific disappeared. In contrast, the leading EOF of NAO-removed 500-hPa heights (Fig. 4b), which accounts for 12.90%, indicates that signals over the North Pacific are prevailing although secondary signals remain over the North Atlantic and Eurasia. The corresponding PCs appear to fluctuate in concert with the NP indices on interdecadal scales.

The NP and NAO indices show a negligible correlation (+0.034) and the frequency properties on decadal/interdecadal scales are also different: spectral peaks at 7.2 yr in the NAO index, which coincide with Rogers's (1984) results, and a broad peak longer than 20 yr in the NP index (Trenberth and Hurrell 1994). The irregular oscillations on those timescales are visible in both series (Figs. 4a and 4b). Results described above suggest that the dominant atmospheric variations over the North Pacific and the North Atlantic are independent phenomena that are either internally generated or forced by oceans. The leading PCs of NP- and NAO-removed fields, however, are not independent of each other because of the significant correlation coefficient (+0.670). This would be attributed to variations neither regressed upon the NAO nor NP indices, and the residual variability is found in the leading EOF of both (i.e., NP and NAO) removed 500-hPa heights (Fig. 4c). The pattern of Fig. 4c represents the EU teleconnection in addition to signals over the polar cap and we therefore interpret that signals over Eurasia in the NP-removed and NAO-removed EOF1s (Figs. 4a and 4b) result from a variability of the EU partially retained in the fields. The leading PCs of both removed fields have no pronounced spectral peak on decadal/interdecadal band.

Since the atmospheric patterns in Figs. 1a and 3 are a mixture of the zonally symmetric and regional components, EOFs are calculated for the zonal mean and the residual 500-hPa height fields (denoted as the ZM and ZM-removed fields, respectively) to understand which fields are responsible for the decadal changes (Fig. 4d). The leading EOF of the ZM height fields (not shown) has a polarity of positive and negative signals in midlatitudes and polar regions while the leading EOF of the ZM-removed fields (Fig. 4d, right panel) represents a horizontal structure similar to Fig. 3. The corresponding PCs of the ZM-removed fields show a larger variability than that of the ZM fields. Most of the decadal-scale variations are evidently attributable to the stationary wave component, although the zonally symmetric component also contributes to the decadal anomalies in part (e.g., early 1970s and 1990s).

Thus Fig. 4 indicates that the spatial characteristic associated with decadal height changes in 1989 (Fig. 1a) is explained not only by the zonally symmetric seesaw between midlatitudes and polar regions but also by the linear combination of the NAO, PNA, and EU teleconnections. In other words, the hemispheric extent of decadal anomalies is consequent upon a complex teleconnection. It is also suggested from time series in Fig. 4 that the sharp transition in 1989 arises from the simultaneous phase shifts of the Pacific interdecadal and Atlantic decadal variations in the atmosphere. The concurrence of two modes is similarly found in winter 1977. Figure 5 shows epoch differences centered on 1977 in 500-hPa heights as in Fig. 1a, but the periods of the epoch are altered to 9 and 4 yr, which may be appropriate to low-frequency variations over the North Pacific and North Atlantic (Fig. 4). As expected, 9-yr differences reveal that the Aleutian low is deepened after 1977, which follows the result by Nitta and Yamada (1989), while 4-yr differences show that the NAO and EU patterns are dominant in addition to the PNA-like anomalies. The latter difference pattern (Fig. 5b) is reminiscent of decadal changes in 1989, except for the sign reversed. The characteristic difference between Figs. 5a and 5b is robust enough even if the periods are changed to 10 and 5 yr, respectively. Height differences with respect to other years that indicate significant shifts in the NAO indices (e.g., 1980 and 1985) show large

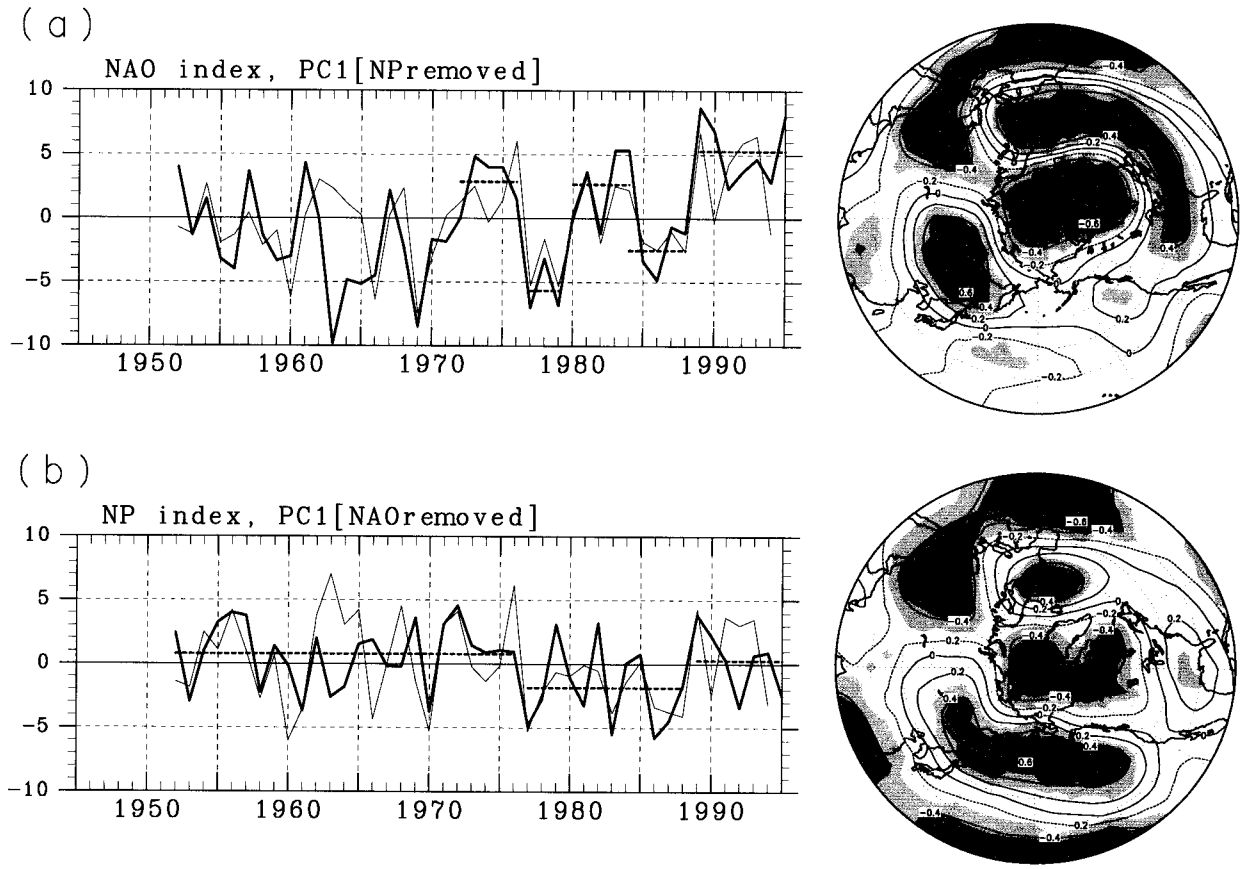

FIG. 4. (a) Spatial pattern of the leading EOF of NP-removed 500-hPa heights in winter (right panel) and its PCs (thin line) superimposed on the NAO indices denoted as the thick line (left panel). The right panel shows correlations as in Fig. 3. Unit of the left panel is hPa for the NAO indices while arbitrary for the leading PCs. Thick dashed lines in the left panel denote mean value for each regime in the NAO

anomalies over only the North Atlantic and Eurasia, unlike Figs. 1a and 5b.

The pattern in Fig. 5b manifests that the shifts in 1989 are not singular, and synchronous phase shifts of two independent modes of variability work to generate such a hemispheric anomalies. In the next subsection, the origin of those quasi-decadal and interdecadal atmospheric variations will be investigated in terms of the coupling between the atmosphere and SSTs.

b. Relationship with tropical/extratropical SST anomalies

For detection of the coupling mode between the atmosphere and SST, the singular value decomposition (SVD) can be used as an analysis tool (e.g., Wallace et al. 1992; Iwasaka and Wallace 1995). The SVD is superior for investigating the covariability in two fields, as much as the canonical correlation analysis (CCA), as described by Bretherton et al. (1992), which gives a detailed description of the SVD analysis. From a viewpoint that low-frequency variations over the North Pacific and North Atlantic may be associated with each ocean basin, the SVD analysis is performed between hemispheric 500-hPa heights and SSTs in the Pacific and Atlantic Oceans separately. This approach may be similar to the SVD analysis of 500-hPa heights and global SSTs with a rotation. In order to examine a dependence of a mode to be obtained on SST variations in the other ocean basins, heterogeneous correlation maps for SST fields are extended to the near-global domain. Although a statistical test for the SVD expansion is not established yet, the significance of the leading SVD modes is evaluated using the Monte Carlo method according to Wallace et al. (1992).

The heterogeneous correlation patterns of the leading SVD between 500-hPa heights and SSTs in the Atlantic Ocean ($S_{\mathrm{Atl}}1$) are shown in Fig. 6. The value of $S_{\mathrm{Atl}}1$ accounts for 33.92% of the total covariance, and the correlation coefficient between expansion coefficients for each field is 0.70. The pattern of $S_{\mathrm{Atl}}1$ in 500-hPa heights is quite similar to Fig. 4a, and significant correlations are found over the Atlantic region, Europe, and the Eurasian continent (Fig. 6a). The correlation map of $S_{\mathrm{Atl}}1$ in Atlantic SSTs (Fig. 6b) reveals a ''sandwich'' pattern, which is known as a pattern in association with the NAO (Lanzante 1984; Wallace et al. 1990). Actually, the expansion coefficients are highly

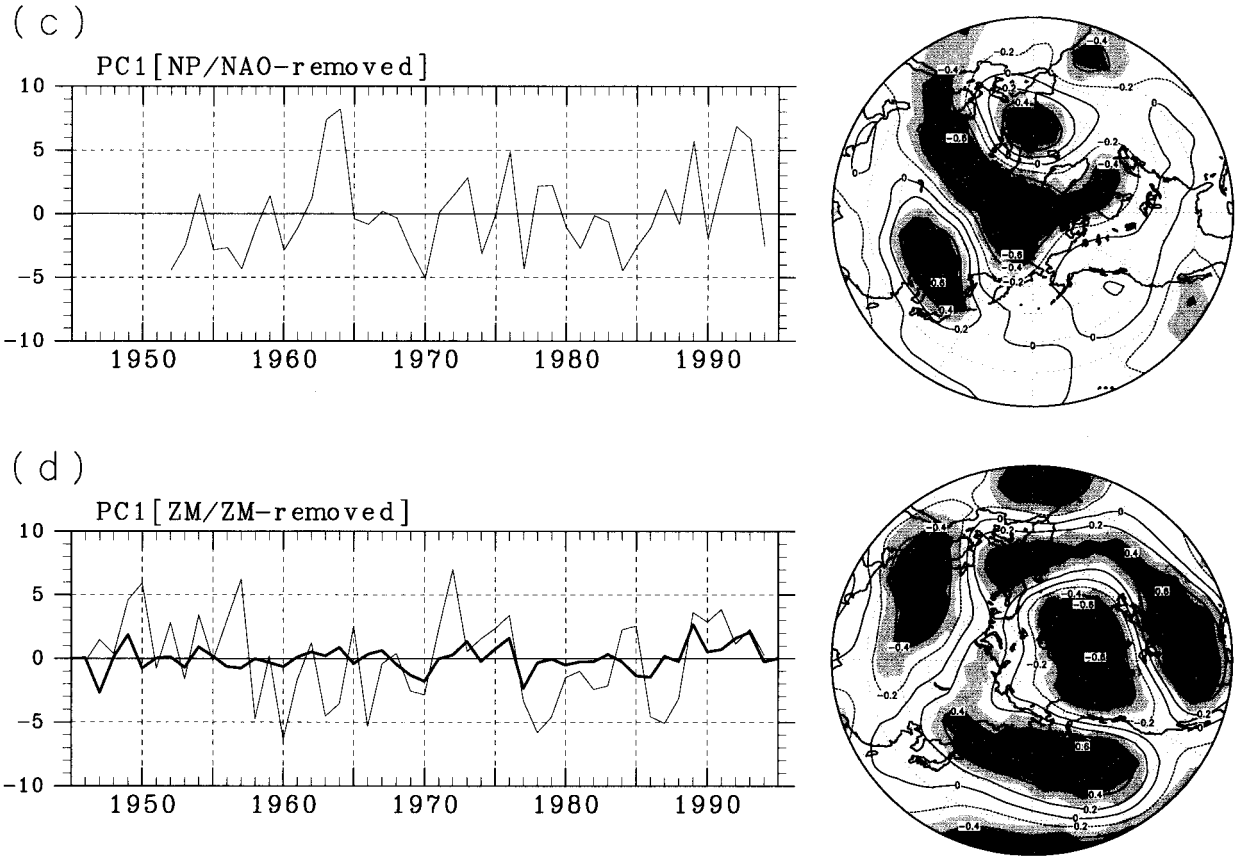

FIG. 4. (*Continued*) indices. (b) As in (a) except for the leading EOF of NAO-removed fields and the PCs shown with the NP indices. (c) As in (a) except for the leading EOF of NP- and NAO- removed fields and the PCs. (d) As in (a) except for the leading EOF of ZM-removed fields and corresponding PCs (thin line), and the leading PCs of zonal mean (ZM) heights (thick line).

correlated with the NAO indices (+0.796 for 500-hPa heights and +0.640 for Atlantic SSTs). The zonally elongated height pattern of $S_{\text{Atl}}1$ is slightly different from dipole anomalies associated with the North Atlantic decadal variability (Deser and Blackmon 1993). Note that the coherent SST fluctuations with the $S_{\text{Atl}}1$ of 500-hPa heights are not found in the tropical Pacific, although SST anomalies show significant correlations in limited regions of the North Pacific.

Suppose that the pattern shown in Fig. 6a has a strong barotropic structure, which is inferred from an analogy with results of the EOF analysis for 500-hPa heights, then the $S_{\text{Atl}}1$ mode could be interpreted from a physical viewpoint as a coupled air–sea variation in the strength of the subtropical jet, surface westerly wind, and SST over the midlatitude Atlantic. When the subtropical jet is weakened with zonally elongated high pressure anomalies over the Altantic, the corresponding weak surface wind may be connected with positive SST anomalies over the midlatitude Atlantic Ocean on the basin scale. This interpretation is supported by Cayan (1992) who investigated the spatial structure for the air–sea heat exchange in the northern oceans.

Results of the significance test for $S_{\text{Atl}}1$ are summarized in Table 1. As in Iwasaka and Wallace (1995), the statistical significance is estimated from the comparison of three quantities: the correlation between the expansion coefficients, the squared covariance fraction (SCF), and the normalized root-mean-squared covariance fraction (NCF) between $S_{\text{Atl}}1$ and 100 realizations of the SVD expansion obtained by using 500-hPa height fields randomly shuffled in the time domain. Here it is assumed that the respective 100 realizations, which may not be a large enough number, form a normal distribution. Mathematical representations for the SCF and NCF are given by Iwasaka and Wallace (1995). As shown in Table 1, it is evident that NCF and the correlation between the expansion coefficients for $S_{\text{Atl}}1$ are significant at the 5% level. However, SCF is less significant, and the small value of the SCF for $S_{\text{Atl}}1$ relative to those for randomized expansions is probably a consequence of the dominance of each individual field by the leading EOFs, as discussed in Wallace et al. (1992).

Figure 7 shows the heterogeneous correlation patterns of the first SVD between 500-hPa heights and Pacific SSTs ($S_{\text{Pac}}1$). The SCF of this mode, which explains over two-thirds of the total covariance field (66.64%), is nearly twice that of $S_{\text{Atl}}1$. Correlations shown later in Fig.

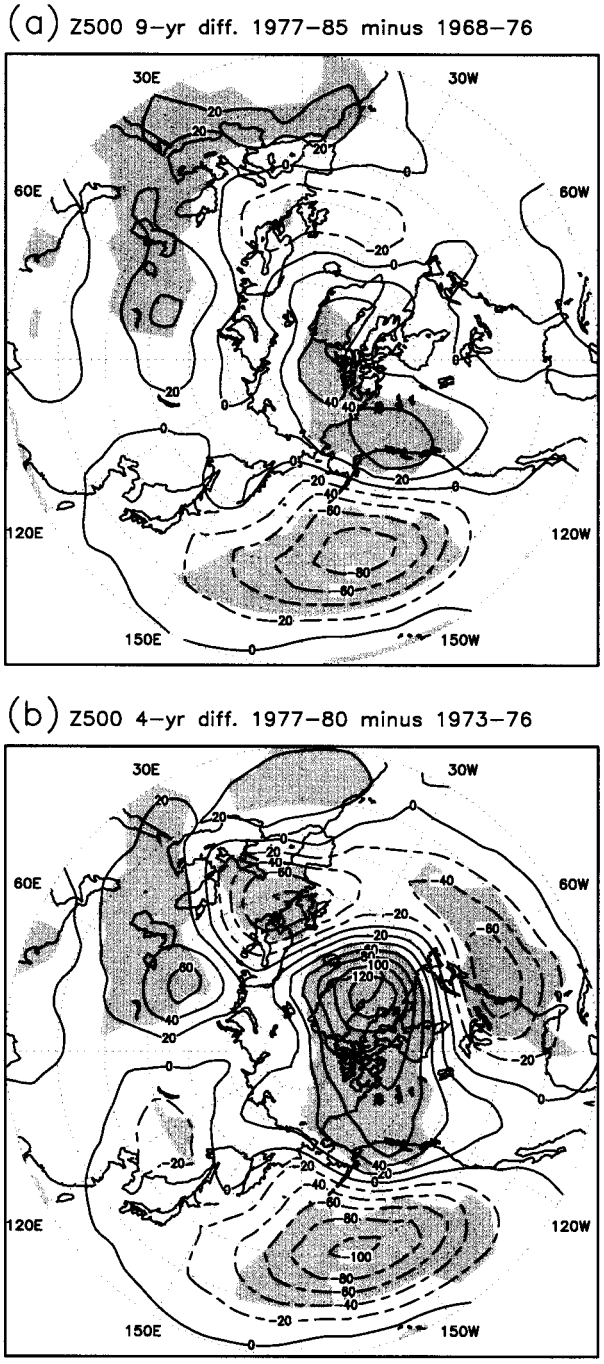

FIG. 5. (a) The 9-yr differences in winter 500-hPa heights from 1977 to 1985 versus 1968 to 1976. (b) As in (a) but the 4-yr differences from 1977 to 1980 versus 1973 to 1976. Contour interval is 20 m, and areas where *t* test exceeds the 5% significance level are shaded.

7 compose a well-known air–sea coupled pattern between the atmosphere and SSTs over the Pacific: the PNA teleconnection, warming in the tropical central-eastern Pacific, and cooling in the central extratropical Pacific. The $S_{\text{Pac}}1$ mode contains two dominant timescales of variability, as shown in Fig. 7c. One is an interannual variation that corresponds to ENSO, another is an ENSO-like interdecadal variability described in previous studies (e.g., Zhang et al. 1997). When the significance test is performed for $S_{\text{Pac}}1$, the result shows that $S_{\text{Pac}}1$ is quite robust (significant at the 1% level) for all three quantities: NCF, SCF, and correlation coefficient (Table 1). This robustness further supports the strong air–sea coupling represented by the $S_{\text{Pac}}1$ mode. It is noted that significant correlations found over a wide area in the SST field suggest that this mode of variability indicates a stronger air–sea coupling over a large area of the Pacific than the $S_{\text{Atl}}1$ mode.

In addition to the correlation patterns between the expansion coefficients for each field, the difference between the percentage of variance explained by the expansion coefficients of one field (equal to the eigenvalue in the usual EOF) and that of another field is also an indicator of the intensity of coupling between two fields. For $S_{\text{Atl}}1$, the percentages for the homogeneous maps are nearly three times larger than those for the heterogeneous maps in both fields: 19.57 and 7.31% in 500-hPa height fields, and 13.52 and 5.87% in the SST field. For $S_{\text{Pac}}1$, on the other hand, percentages of variance for a field are less than twice of those explained by other fields. Thus the $S_{\text{Atl}}1$ mode represents a relatively weak coupling to the Pacific counterpart, $S_{\text{Pac}}1$.

Although the mechanisms of interdecadal and decadal variations in the Pacific and North Atlantic Oceans are still under debate, the SVD expansions presented here further support that the decadal atmospheric changes over the Northern Hemisphere consist of two independent modes of variability which respectively result from the Pacific and Atlantic atmosphere–ocean coupling.

c. Changes in surface temperature and snow cover

It is reported that the atmospheric teleconnections often accompany certain changes in land surface climate (Ting et al. 1996; Hurrell 1996). Figure 8a shows 6-yr differences in surface air temperature and SSTs calculated in a manner similar to Fig. 1. As in Fig. 1, large areas exceed the 5% significance level by the *t* test. It is apparent that the significant warming occurred over most of the Eurasian continent, especially Europe and eastern Eurasia, where the warm air is advected from the south accompanied by the NAO and EU patterns (Fig. 1a). Also, cooling is found over Alaska and northeastern Canada. Extratropical SSTs reveal a warming (<1 K) between 30° and 60°N in the Pacific and Atlantic Oceans. It is inferred from Fig. 8a that the surface temperatures reveal a decadal-scale change in relation to the atmospheric shifts in 1989. In particular, surface temperature variations over the warming regions in the Eurasian continent (Fig. 8b) represent a decadal variability similar to that in the NAO indices (Fig. 4a). These are consistent with results by Hurrell (1996) who showed that most of the variations in Eurasian surface

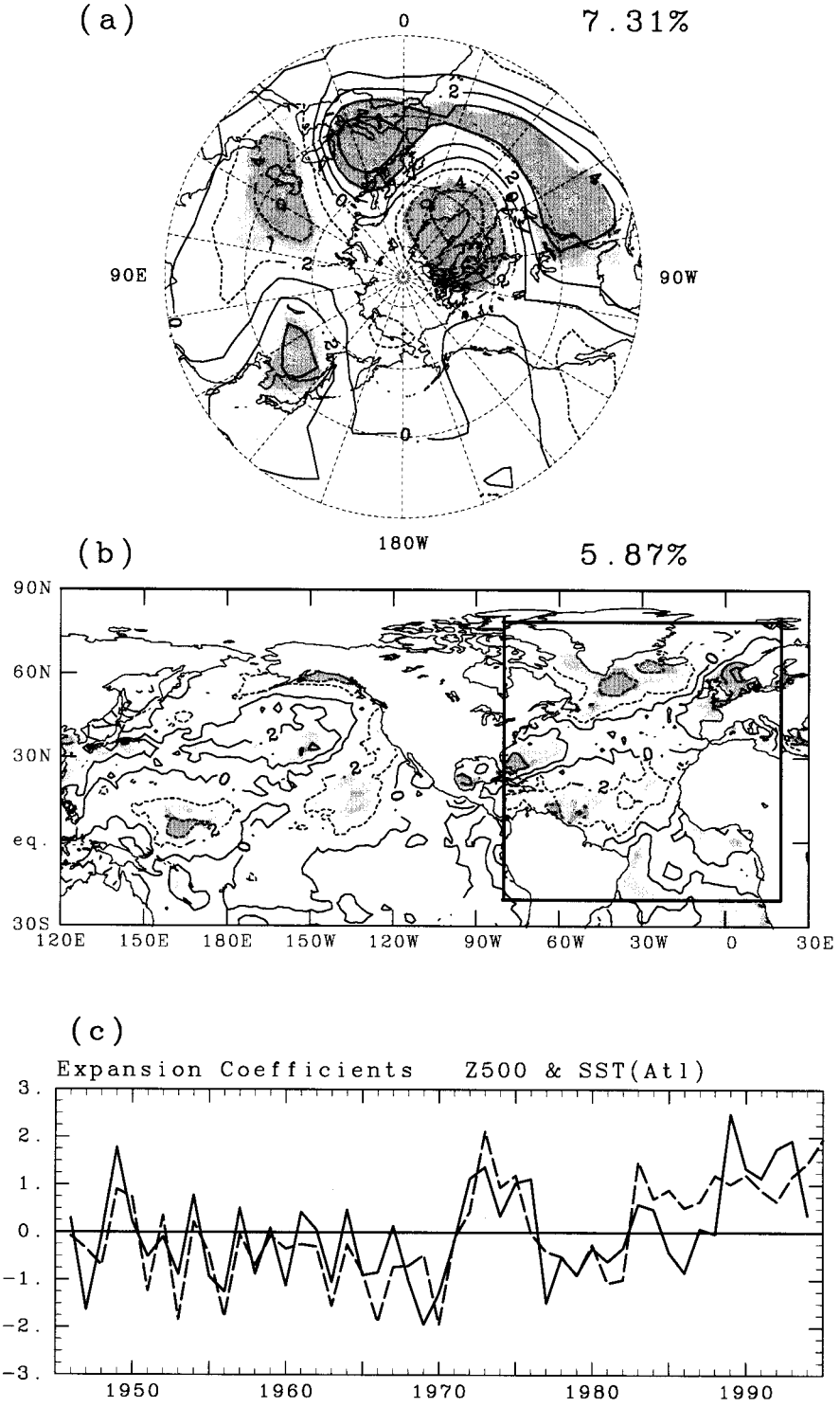

FIG. 6. Heterogeneous correlation patterns for the leading mode in the SVD expansion of (a) 500-hPa heights and (b) SST in the Atlantic Ocean, and (c) expansion coefficients of 500-hPa heights (solid line) and Atlantic SSTs (broken line). It is noted that the correlations in the SST field are expanded to the Pacific Ocean, although SST anomalies in the Atlantic only [framed area in (b)] are used for the SVD expansion. The SCF of this mode accounts for 33.92%, while the correlation coefficient is 0.70. (a) and (b) Contour intervals are 0.2, while negative values are dashed. Light (dark) shading denotes regions in which correlation coefficients exceed the 5% (1%) significance level. The percentage of variances explained by the expansion coefficients of the other field is written on the upper-right corner of each map.

TABLE 1. Results of 100 SVD expansions of 500-hPa height and Atlantic (Pacific) SSTs, in which 500-hPa height field is randomly replaced in time sequences. Quantities for $S_{Atl}1$ ($S_{Pac}1$) are also presented.

	NCF	SCF	*r*
Atlantic Ocean			
$S_{Atl}1$	8.091	33.916	0.700
100 realizations			
Highest	8.129	44.167	0.791
Fifth	7.463	40.605	0.692
Mean	6.057	29.648	0.598
Std dev	0.740	5.064	0.060
Pacific Ocean			
$S_{Pac}1$	27.404	66.642	0.785
100 realizations			
Highest	22.149	65.277	0.572
Fifth	17.958	58.640	0.549
Mean	14.066	42.238	0.471
Std dev	2.382	8.722	0.047

temperature are explained by the NAO. The temperature time series in Fig. 8b also indicate the upward trend as shown by Wallace et al. (1995)

It may be possible that changes in the lower-tropospheric atmosphere affect surface air temperature anomalies, and also the reverse relationship may be possible: changes in surface air temperature force the atmosphere to produce anomalies such as in Fig. 1. Perhaps snow fluctuations in the Northern Hemisphere play an important role in the coupling between the atmosphere and the land surface temperature field, because of a cumulative interaction between the surface temperature and snow cover. Therefore, an attempt to find the mechanisms for shifts in the atmosphere in winter 1989 is expanded to the analysis of observed snow cover anomalies.

Atmospheric shifts described in section 3 are presented in winter mean fields. It is considered that the atmospheric variability of longer than the season is difficult to explain only by the internal dynamics within the atmosphere. Thus some components, regardless of internal or external variables of the climate system, having longer memory than the atmosphere may have forced the atmospheric change in winter 1989. Changes in the snow and associated land surface conditions are potential components for atmospheric changes as important as those in SSTs; therefore, it is meaningful to investigate the snow cover variability in the Northern Hemisphere.

The satellite-derived snow cover data described in section 2 are used for the analysis. Before investigating temporal variations, time-mean statistics are briefly described. In the Northern Hemisphere, permanent snow is found in a small region over Greenland. Even over Siberia and Alaska, snow covers less than 25% of the ground in summer. Snow extent (hereafter referred to as the SE) over the Northern Hemisphere land in winter (4467.14×10^4 km^2) is nearly 7 times larger than that in summer (648.72×10^4 km^2). Compared to this dominant seasonal variation, the interannual variability has small amplitude. On a seasonal basis, the interannual variability is large over regions corresponding to the edges of climatological states. Groisman et al. (1994) called those regions ''snow transient regions'' and regarded them as the center of action in interannual fluctuations of snow cover.

To focus on the changes in 1989, snow cover differences in winter (December–February) are taken between 3-yr averages for 1989–91 and 1986–88 (Fig. 9a). Because the data after 1991 are not available, each 3 yr before and after 1989 are used to calculate differences, which may be influenced by year-to-year variations. The pattern of differences indicates that the winter snow cover decreased after 1989 over Europe, China, and Canada. Decreases of snow cover over these areas continues into spring (not shown). It is noted that those areas correspond to warming regions in the middle atmosphere (Fig. 1b). Furthermore, similar differences, but with a season-precedent snow cover, show different large-scale anomalies (Fig. 9b). Deficiencies of snow cover in autumn are dominant over the midlatitude Eurasian continent and North America. The decrease of the SE over the Northern Hemisphere amounts to -216.00×10^4 km^2 in autumn, and is larger than that in the following winter (-100.48×10^4 km^2).

In order to calculate an SE time series that shows the temporal variation, Northern Hemisphere land is divided into seven regions according to the seasonal cycle, variability, and 3-yr difference patterns. Although this may be subjective, homogeneity of snow fluctuation in each area is taken into account in dividing the area. Regional extent and reference name for each area are shown in Fig. 10a.

Time series of the SE for area 2 (eastern Eurasia) are depicted in Fig. 10b. Only the SE time series over eastern Eurasia are shown here, because the variations of the seasonal SE in eastern Eurasia are probably related to the changes in surface temperatures over eastern Eurasia (Fig. 8) coupled with the atmospheric shifts. That is, Fig. 10b indicates that the September–November SE over eastern Eurasia is remarkably decreased in 1988 prior to the atmospheric change in winter 1989. In contrast, the SE in autumn is increased conspicuously in 1976 preceding the changes in the atmosphere in 1977, with the reverse sign to what occurred in 1989 (Fig. 9b). Anomalies of the SE in 1988 and 1976 amount to -1.344×10^6 km^2 and 1.773×10^6 km^2, respectively, and both anomalies exceed twice the autumn SE variability for 1972–91 (2 SD = $\pm 1.342 \times 10^6$ km^2). The SE time series in autumn shows weak negative anomalies after the great decrease in 1989, and these coincide with the result of 3-yr differences in snow cover (Fig. 9b). There are no coherent fluctuations between the autumn SE anomalies in eastern Eurasia and those in other areas. However, negative SE anomalies are found in

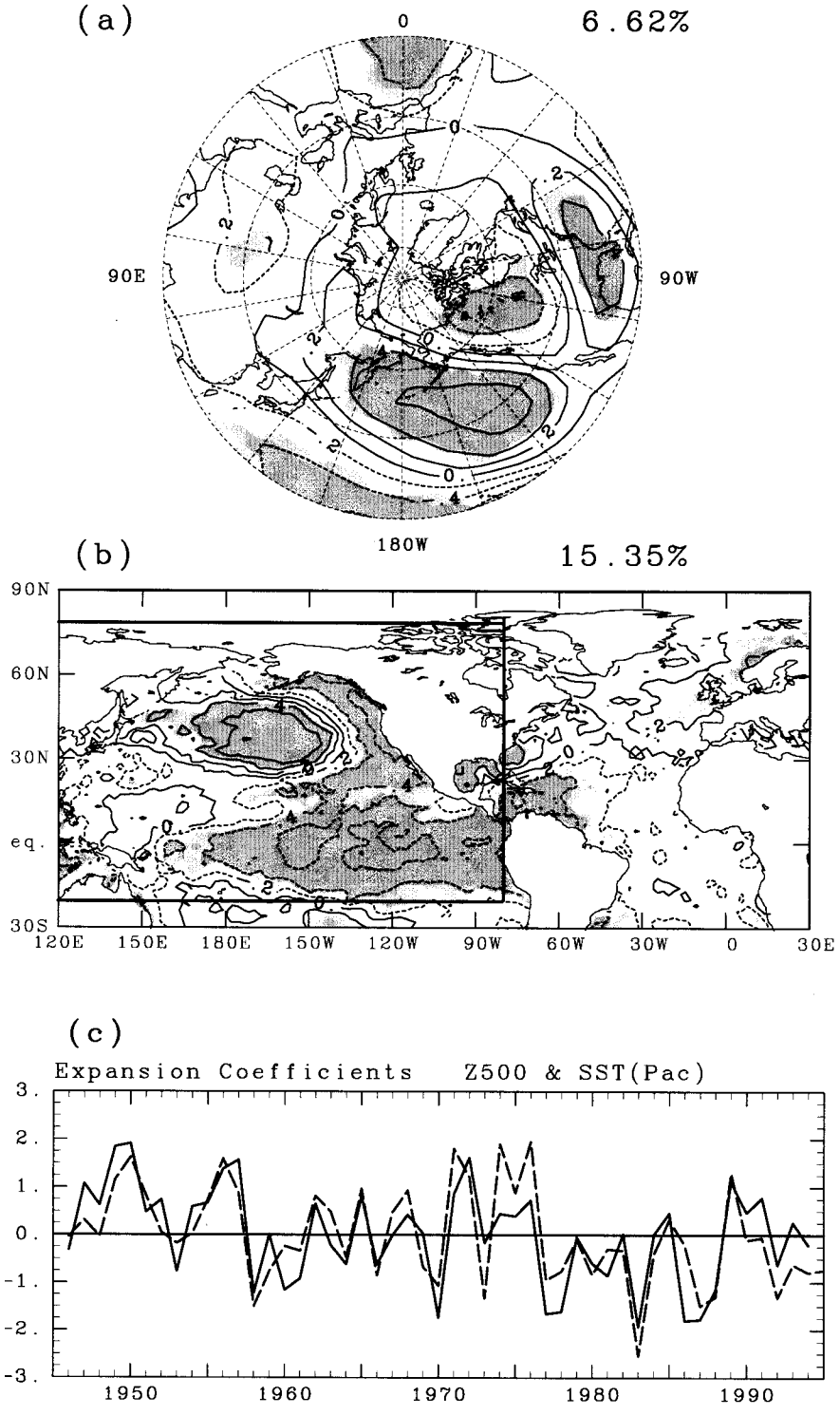

FIG. 7. Same as in Fig. 6 except for results of the first mode in the SVD expansion of 500-hPa heights and Pacific SSTs. The SCF and correlation coefficient are, respectively, 66.64% and 0.78.

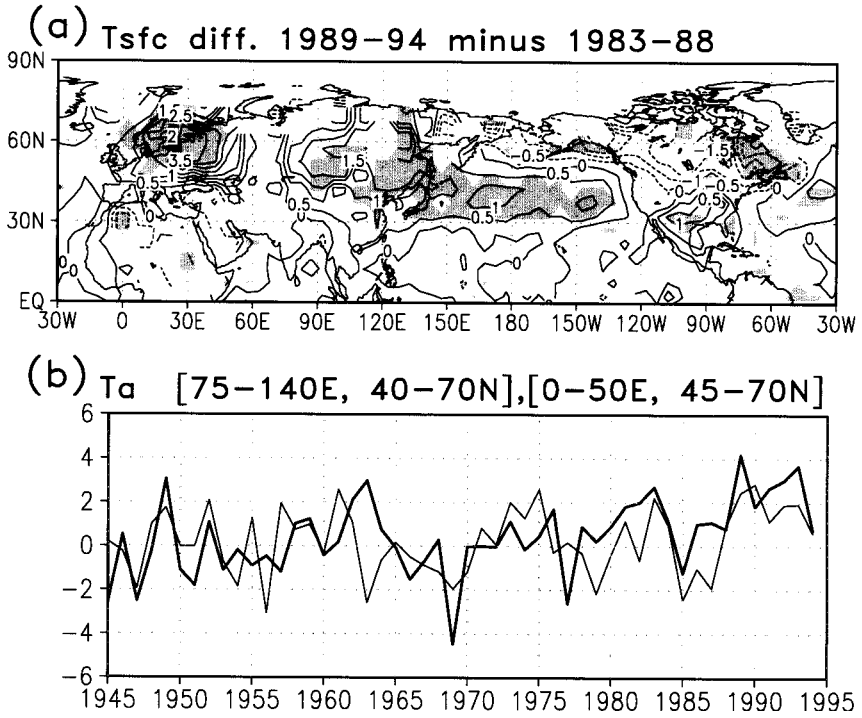

FIG. 8. (a) Same as in Fig. 1 except for differences in combined surface temperature (air temperature over lands and SST over oceans). Contour interval is 0.5 K. (b) Surface air temperature anomalies for 1945–95 averaged over 40°–70°N, 75°–140°E (thick line) and 45°–70°N, 0°–50°E (thin line). Unit is K.

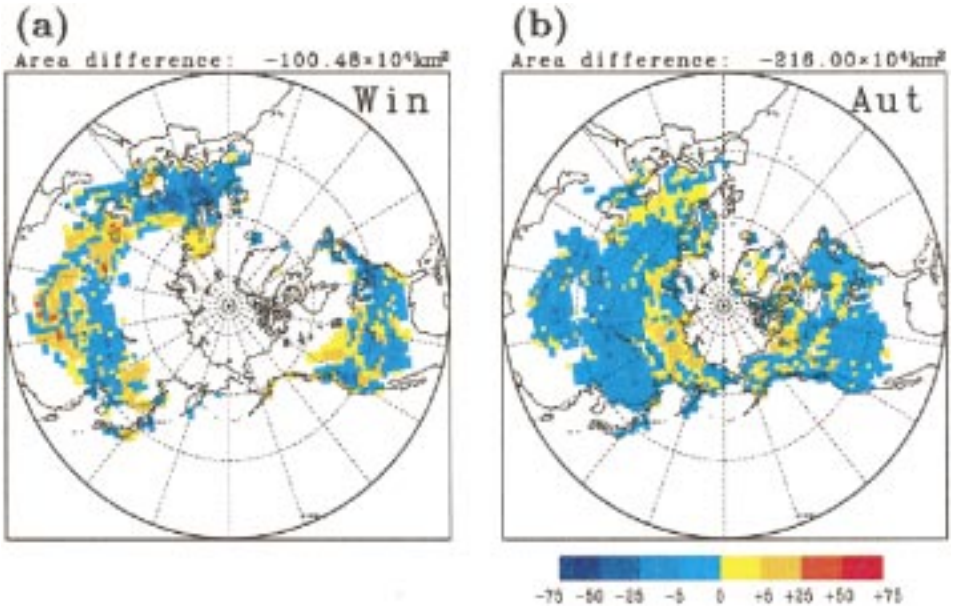

FIG. 9. (a) Differences in winter snow cover between 1989–91 and 1986–88, and (b) same as in (a) except for preceding autumn (1988–90 minus 1985–87). Units are fraction (%). Snow extent difference over the hemisphere is shown at the top of each figure.

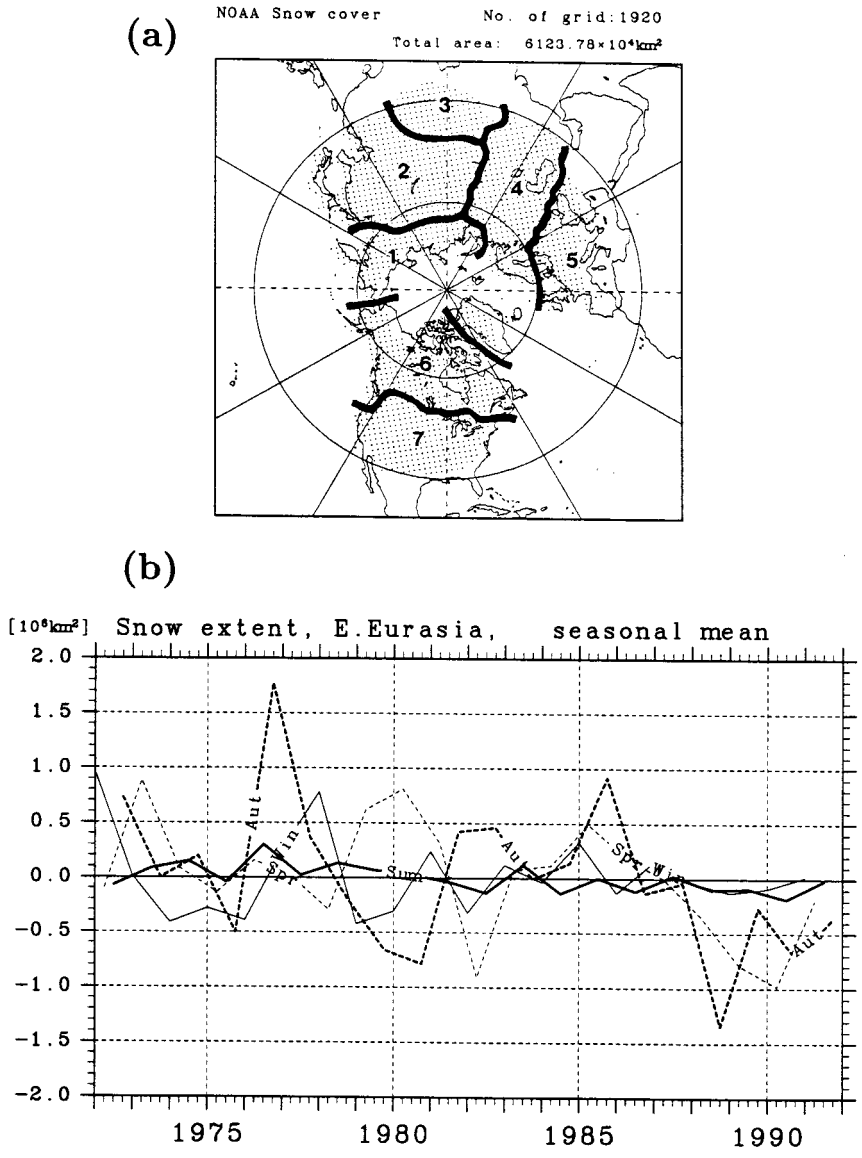

FIG. 10. (a) Regional division for calculations of the SE. Dots denote grid points where the weekly observations have reported the presence of snow at least once in January. Reference names for each region in the figure are as follows: 1) Siberia, 2) eastern Eurasia, 3) Tibetan Plateau, 4) western Eurasia, 5) Europe, 6) northern North America, 7) southern North America. (b) Time series of the seasonally averaged SE over eastern Eurasia. Units are 10^6 km^2, and the solid (broken) thick line and the solid (broken) thin line represent the SE for summer (autumn) and winter (spring), respectively.

Europe in winter 1989, and in Siberia in summer after 1988. The former is consistent with warming over Europe (Fig. 8), and the latter corresponds to the recent decrease in summer ice cover in the offshore region of Siberia (Maslanik et al. 1996).

The relationship between the variability of the autumn SE in eastern Eurasia and that of the atmospheric circulation is confirmed by the correlation pattern between the autumn SE in eastern Eurasia (Fig. 10b) and 500-hPa heights in successive winters (Fig. 11). The pattern shown in Fig. 11 consists not only of the local negative correlations over the Eurasian continent but also of the remote negative correlations over broad regions of midlatitudes, and positive correlations in the polar region. This pattern resembles Fig. 1a and Figs. 3 and suggests that the large negative (positive) anomalies in autumn SE act as a heating (cooling) source through the albedo effect.

Though the autumn SE in eastern Eurasia is coherent with the atmospheric circulation in winter, the snow anomalies in autumn 1976 and 1988 are like pulses in contrast to the continuous anomalies in the atmosphere

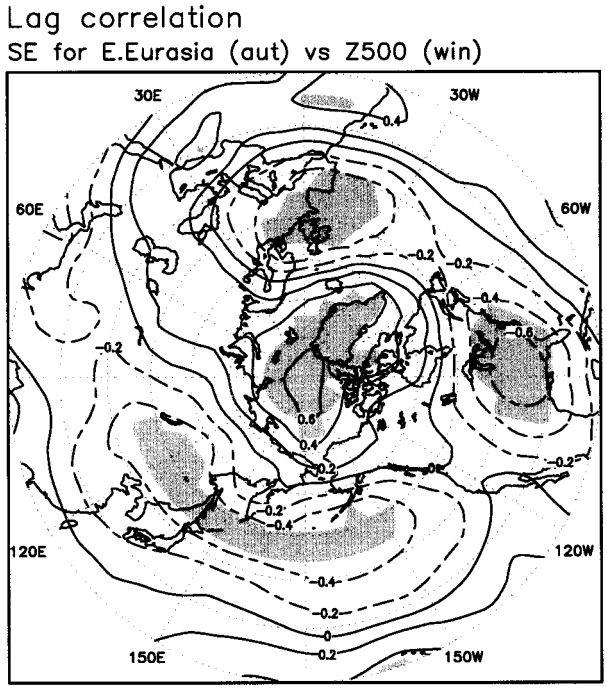

FIG. 11. Correlation of September–November SE over eastern Eurasia with 500-hPa heights in the succeeding winter for 1972 to 1991. Contour interval is 0.2, and negative values are dashed. Values significant at the 5% level using *t* test are shaded.

after winter 1977 and 1989. Snow is thought to be an internal variable of climate; therefore, it is likely that the peculiar snow anomalies in autumn in eastern Eurasia may have a role as an *amplifier* for the atmospheric shifts. Moreover, the above analysis does not give the answer if the Eurasian snow anomaly affects the mid- and high-latitude atmosphere in the opposite hemisphere (i.e., Atlantic sector), although there is a significant statistical relationship (Fig. 11). Results in Watanabe and Nitta (1998), in which these questions are investigated further by using numerical simulations with an AGCM, support the inference above, the importance of snow anomalies as an amplifier.

5. Summary and discussion

This study has attempted to clarify the large-scale structure of decadal changes in the Northern Hemisphere atmosphere in winter 1989. Although these atmospheric changes have been partially reported by several earlier studies, further insight on the three-dimensional structure and temporal characteristics of the changes in atmosphere, sea surface temperature, and snow cover were examined.

Analyses of the atmospheric fields show that changes in 1989 are a decadal-scale shift in winter-mean states and have significant features: the dipole pattern between midlatitudes with positive geopotential height anomalies and polar regions with negative height anomalies after 1989 throughout the troposphere and lower stratosphere with the strong equivalent barotropic structure, corresponding weakening of the subtropical jet and strengthened polar night jet, and the warming and cooling in surface air temperatures over Eurasia and the North Atlantic, respectively. Some of these characteristics are consistent with previous findings.

As mentioned in section 3, the dipole structure in SLP, as in Fig. 1d, reveals a well-known pattern from previous studies. For example, Bjerknes (1964) found that the north–south seesaw in the SLP field was dominant in interdecadal changes of surface climate in the North Atlantic during the early twentieth century. Wallace and Gutzler (1981) concluded that the dipole anomalies in SLP are one of the most feasible patterns in the monthly mean atmospheric field, like the PNA and NAO observed in the middle troposphere.

Decadal-scale height anomalies synchronized with Fig. 1 can be also seen at the 10-hPa level (not shown), which have a pattern similar to that in SLP. This dipole pattern in the stratosphere is known to appear in association with the equatorial quasi-biennial oscillation (QBO) (Holton and Tan 1980). In the case of QBO-related anomalies, the dipole pattern is explained by changes in the vertical penetration of stationary waves into the stratosphere that occur by meridional shifts of the critical latitude, in which the zonal mean flow vanishes, depending on the phase of the stratospheric QBO. We also examined changes in Eliasen–Palm (E–P) fluxes concerning the decadal shift in 1989; however, they showed few anomalies in the stratosphere. The stratospheric dipole accompanied by changes in the polar vortex is often found in association with the tropospheric dipole (Kitoh et al. 1996). Thompson and Wallace (1998) showed that the zonally symmetric component in the dipole is a coupled variation between the troposphere and stratosphere while some regional patterns such as the NAO are confined in the troposphere.

The decadal-scale height anomalies in the troposphere are explained by a linear combination of three types of teleconnections, namely, the NAO, PNA, and EU patterns. The decadal shifts in winter 1989, especially their abruptness, are attributed to a phase matching of low-frequency atmospheric variations over the North Pacific and the North Atlantic. Their spatial and temporal characteristics are detected by the EOFs of 500-hPa heights. Our findings and the interpretation for origins of such variations are consistent with results of Ting et al. (1996), who investigated the interannual-to-decadal changes in the zonal mean flow during 1947–94. They used a zonal mean flow as a key variable and concluded that the extratropical height anomalies are largely explained by changes in zonal mean flow nearly independent of the tropical forcing, except for the North Pacific atmosphere where the influence of the Tropics is prevailing. As referred to in their discussion, changes in zonal flow over the Atlantic and the Eurasian continent are presumably induced from the recurrent NAO pattern.

Although the atmosphere may internally produce multiyear fluctuations (James and James 1989), low-frequency atmospheric variations over the North Pacific and Atlantic appear to be a decadal and interdecadal modes inherent in the atmosphere–ocean system. The SVD expansion for height and SST anomalies strongly suggests that the decadal changes over the North Pacific are generally corresponding to the Pacific interdecadal variations (Nitta and Yamada 1989, among others). Some studies (Trenberth and Hurrell 1994; Graham 1994) have regarded the mode as a coupled air–sea variability driven by changes in tropical SSTs. Recently several reports, however, showed that there is a decadal variability independent of the changes in tropical Pacific SSTs (Deser and Blackmon 1995; Nakamura et al. 1997). Actually, the weakening of the Aleutian low in the 1990s (Fig. 1d) is discrepant to the recent ENSO-like condition of the equatorial Pacific (Trenberth and Hoar 1996).

While the quasi-decadal atmospheric variations over the North Atlantic reveal the north–south dipole, it is ambiguous that they are exactly projected on the Atlantic decadal variations (Deser and Blackmon 1993) because of two reasons: differences in spatial pattern and periodicity. The former implies that decadal height anomalies do not reveal the classic NAO as in the Atlantic decadal variability because subtropical anomalies are zonally elongated. On the other hand, the periodicity dominant in the NAO indices (Fig. 4a) is about 7.2 yr, which is shorter than that of the Atlantic decadal variability of about 12 yr as shown by Deser and Blackmon. Mann and Park (1994) mentioned that both 7–8- and 11–12-yr periods are significant in the NAO of surface air temperatures.

An analysis of snow cover derived from NOAA satellites shows that the snow extent in eastern Eurasia was remarkably deficient in autumn 1988 and sufficient in autumn 1976, and their magnitudes of anomaly were twice as large as the range of interannual variability in the Eurasian snow extent. These results implicate that the snow extent anomalies in autumn may play an important role as a precursor of large atmospheric changes in winters 1977 and 1989. The snow extent anomalies in autumn 1976 and 1988 are, however, not persistent on the decadal scale, but behave rather like pulses. Thus, this observational evidence suggests that large anomalies in the autumn Eurasian snow cover may act as an amplifier to the extratropical atmosphere to be changed in the succeeding winter. With AGCM integrations, Watanabe and Nitta (1998) examined the relative impact of autumn snow anomalies versus tropical and extratropical SST anomalies on the atmospheric circulation. Their results, that the Eurasian snow anomaly in autumn reproduced dipole height anomalies similar to those observed in winter 1989 with a considerable amplitude, reinforce our inference that the Eurasian snow anomalies force the atmosphere as well as SST anomalies. The possible causes of snow anomalies in autumn are not obvious and are currently being investigated.

Acknowledgments. The authors are grateful to Drs. M. Kimoto and H. Nakamura, and two anonymous reviewers for their comments on an earlier version of the manuscript. We also thank Drs. R. Kawamura, H. Koide, and K. Kodera for stimulating discussions. This work was partially supported by a Grant-in-Aid for Scientific Research from the Ministry of Education, Science, and Culture of Japan.

REFERENCES

Barnston, A. G., and R. E. Livezey, 1987: Classification, seasonality and persistence of low-frequency atmospheric circulation patterns. *Mon. Wea. Rev.,* **115,** 1083–1126.

Bjerknes, J., 1964: Atlantic air-sea interaction. *Advances in Geophysics,* Vol. 10, Academic Press, 1–82.

Bretherton, C. S., C. Smith, and J. M. Wallace, 1992: An intercomparison of methods for finding coupled patterns in climate data. *J. Climate,* **5,** 541–560.

Cayan, D. R., 1992: Latent and sensible heat flux anomalies over the northern oceans: The connection to monthly atmospheric circulation. *J. Climate,* **5,** 354–369.

Cheng, X., G. Nitsche, and J. M. Wallace, 1995: Robustness of low-frequency circulation patterns derived from EOF and rotated EOF analysis. *J. Climate,* **8,** 1709–1713.

Deser, C., and M. Blackmon, 1993: Surface climate variations over the North Atlantic Ocean during winter: 1900–1989. *J. Climate,* **6,** 1743–1753.

——, and ——, 1995: On the relationship between tropical and North Pacific sea surface temperature variations. *J. Climate,* **8,** 1677–1680.

Graham, N. E., 1994: Decadal-scale climate variability in the tropical and North Pacific during the 1970s and 1980s: Observations and model results. *Climate Dyn.,* **10,** 135–162.

Groisman, P. Y., T. R. Karl, R. W. Knight, and G. L. Stenchikov, 1994: Changes of snow cover, temperature, and radiative heat balance over the Northern Hemisphere. *J. Climate,* **7,** 1633–1656.

Holton, J. R., and H. C. Tan, 1980: The influence of the equatorial quasi-biennial oscillation on the global circulation at 50 mb. *J. Atmos. Sci.,* **37,** 2200–2208.

Hurrell, J. W., 1995: Decadal trends in the North Atlantic oscillation: Regional temperatures and precipitation. *Science,* **269,** 676–679.

——, 1996: Influence of variations in extratropical wintertime teleconnections on Northern Hemisphere temperature. *Geophys. Res. Lett.,* **23,** 665–668.

Iwasaka, N., and J. M. Wallace, 1995: Large scale air sea interaction in the Northern Hemisphere from a view point of variations of surface heat flux by SVD analysis. *J. Meteor. Soc. Japan,* **73,** 781–794.

James, I. N., and P. M. James, 1989: Ultra-low-frequency variability in a simple atmospheric circulation model. *Nature,* **342,** 53–55.

Jones, P. D., S. C. B. Raper, R. S. Bradley, H. F. Diaz, P. M. Kelly, and T. M. Wigley, 1986: Northern Hemisphere surface air temperature variations: 1851–1984. *J. Climate Appl. Meteor.,* **25,** 161–179.

Kawamura, R., 1994: A rotated EOF analysis of global sea-surface temperature variability with interannual and interdecadal scales. *J. Phys. Oceanogr.,* **24,** 707–715.

Kimoto, M., and M. Ghil, 1993: Multiple flow regimes in the Northern Hemisphere winter. Part I: Methodology and hemispheric regimes. *J. Atmos. Sci.,* **50,** 2625–2643.

Kitoh, A., H. Koide, K. Kodera, S. Yukimoto, and A. Noda, 1996: Interannual variability in the stratospheric-tropospheric circu-

lation in a coupled ocean–atmosphere GCM. *Geophys. Res. Lett.,* **23,** 543–546.
Kushnir, Y., 1994: Interdecadal variations in North Atlantic sea surface temperature and associated atmospheric conditions. *J. Climate,* **7,** 141–157.
——, and J. M. Wallace, 1989: Low-frequency variability in the Northern Hemisphere winter: Geographical distribution, structure, and time-scale dependence. *J. Atmos. Sci.,* **46,** 3122–3142.
Lanzante, J. R., 1984: A rotated eigenanalysis of the correlation between 700 mb heights and sea surface temperatures in the Pacific and Atlantic. *Mon. Wea. Rev.,* **112,** 2270–2280.
Latif, M., and T. P. Barnett, 1994: Causes of decadal climate variability over the North Pacific and North America. *Science,* **266,** 634–637.
——, and ——, 1996: Decadal climate variability over the North Pacific and North America: Dynamics and predictability. *J. Climate,* **9,** 2407–2423.
Mann, M. E., and J. Park, 1994: Global-scale modes of surface temperature variability on interannual to century timescales. *J. Geophys. Res.,* **99,** 25 819–25 833.
Maslanik, J. A., M. C. Serreze, and R. G. Barry, 1996: Recent decreases in Arctic summer ice cover and linkages to atmospheric circulation anomalies. *Geophys. Res. Lett.,* **23,** 1677–1680.
Nakamura, H., G. Lin, and T. Yamagata, 1997: Decadal climate variability in the North Pacific during the recent decades. *Bull. Amer. Meteor. Soc.,* **78,** 2215–2225.
Nitta, T., and S. Yamada, 1989: Recent warming of tropical sea surface temperature and its relationship to the Northern Hemisphere circulation. *J. Meteor. Soc. Japan,* **67,** 375–383.
North, G., T. Bell, R. Cahalan, and F. Moeng, 1982: Sampling errors in the estimation of empirical orthogonal functions. *Mon. Wea. Rev.,* **110,** 699–706.
Richman, M. B., 1986: Rotation of principal components. *J. Climatol.,* **6,** 293–335.
Rogers, J. C., 1984: The association between the North Atlantic oscillation and the Southern Oscillation in the Northern Hemisphere. *Mon. Wea. Rev.,* **112,** 1999–2015.
Tachibana, Y., M. Honda, and K. Takeuchi, 1996: The abrupt decrease of the sea ice over the southern part of the sea of Okhotsk in 1989 and its relation to the recent weakening of the Aleutian low. *J. Meteor. Soc. Japan,* **74,** 579–584.
Tanaka, H. L., R. Kanohgi, and T. Yasunari, 1996: Recent abrupt intensification of the northern polar vortex since 1988. *J. Meteor. Soc. Japan,* **74,** 947–954.
Tanimoto, Y., N. Iwasaka, K. Hanawa, and Y. Toba, 1993: Characteristic variations of sea surface temperature with multiple timescales in the North Pacific. *J. Climate,* **6,** 1153–1160.
Thompson, D. W. J., and J. M. Wallace, 1998: The Arctic oscillation signature in the wintertime geopotential height and temperature fields. *Geophys. Res. Lett.,* **25,** 1297–1300.
Ting, M., M. P. Hoerling, T. Xu, and A. Kumar, 1996: Northern Hemisphere teleconnection patterns during extreme phases of the zonal-mean circulation. *J. Climate,* **9,** 2614–2633.
Trenberth, K. E., 1990: Recent observed interdecadal climate changes in the Northern Hemisphere. *Bull. Amer. Meteor. Soc.,* **71,** 988–993.
——, and D. A. Paolino, 1981: Characteristic patterns of variability of sea level pressure in the Northern Hemisphere. *Mon. Wea. Rev.,* **109,** 1169–1189.
——, and J. W. Hurrell, 1994: Decadal atmosphere–ocean variations in the Pacific. *Climate Dyn.,* **9,** 303–319.
——, and T. J. Hoar, 1996: The 1990–1995 El Niño–Southern Oscillation event: Longest on record. *Geophys. Res. Lett.,* **23,** 57–60.
Wallace, J. M., and D. S. Gutzler, 1981: Teleconnections in the geopotential height field during the Northern Hemisphere winter. *Mon. Wea. Rev.,* **109,** 784–812.
——, C. Smith, and Q. Jiang, 1990: Spatial patterns of atmosphere–ocean interaction in the northern winter. *J. Climate,* **3,** 990–998.
——, ——, and C. S. Bretherton, 1992: Singular value decomposition of wintertime sea surface temperature and 500-mb height anomalies. *J. Climate,* **5,** 561–576.
——, Y. Zhang, and J. A. Renwick, 1995: Dynamic contribution to hemispheric mean temperature trends. *Science,* **270,** 780–783.
Walsh, J., W. Chapman, and T. Shy, 1996: Recent decrease of sea level pressure in the central Arctic. *J. Climate,* **9,** 480–486.
Watanabe, M., and T. Nitta, 1998: Relative impacts of snow and sea surface temperature anomalies on an extreme phase in the winter atmospheric circulation. *J. Climate,* **11,** 2837–2857.
Wiesnet, D. R., C. F. Ropelewski, G. J. Kukla, and D. A. Robinson, 1987: A discussion of accuracy of NOAA satellite-derived global snow cover measurements. *Large Scale Effects of Seasonal Snow Cover,* IHAS Publ. 166, 291–304.
Yonetani, T., 1992: Discontinuous changes of precipitation in Japan after 1900 detected by the Lepage test. *J. Meteor. Soc. Japan,* **70,** 95–104.
Zhang, Y. Z., J. M. Wallace, and D. S. Battisti, 1997: ENSO-like interdecadal variability: 1900–1993. *J. Climate,* **10,** 1004–1020.